

A differential equations approach to l_1 -minimization with applications to array imaging

Miguel Moscoso* Alexei Novikov† George Papanicolaou‡ Lenya Ryzhik§

October 10, 2018

Abstract

We present an ordinary differential equations approach to the analysis of algorithms for constructing l_1 minimizing solutions to underdetermined linear systems of full rank. It involves a relaxed minimization problem whose minimum is independent of the relaxation parameter. An advantage of using the ordinary differential equations is that energy methods can be used to prove convergence. The connection to the discrete algorithms is provided by the Crandall-Liggett theory of monotone nonlinear semigroups. We illustrate the effectiveness of the discrete optimization algorithm in some sparse array imaging problems.

1 Introduction

We consider the solution of large underdetermined linear systems of equations $Ax = y$ where $A \in \mathbb{R}^{m \times n}$ is a given matrix, $y \in \mathbb{R}^m$ is a known vector of $m \ll n$ measurements, and $x \in \mathbb{R}^n$ is the unknown signal or image to be estimated. We assume that A has full rank equal to m . We want to find the solutions of this system with minimal l_1 norm $\|x\|_{l_1}$,

$$\min \|x\|_{l_1}, \quad \text{subject to } y = Ax. \quad (1.1)$$

Our motivation is array imaging problems, which is an application discussed in this paper, but such sparsity inducing constrained minimization problems, where the l_1 norm of the solution vector is used, arise in many other applications in signal and image processing [14].

A lot of research has been devoted to developing algorithms for solving efficiently (1.1) and its relaxed form

$$\min_x \left\{ \tau \|x\|_{l_1} + \frac{1}{2} \|y - Ax\|^2 \right\}. \quad (1.2)$$

Here, and throughout the paper, $\|q\|$ denotes the l_2 -norm of a vector q . In (1.2), the exact constraint $y = Ax$ is relaxed so as to take into account possible measurement noise, and τ is a positive real parameter that promotes sparse solutions when it is large enough.

The iterative shrinkage-thresholding algorithm (ISTA) is the usual gradient descent method applied to (1.2). It has been used in many different applications with great success, such as [12, 16–18, 25, 47], just to mention a few. The ISTA algorithm generates a sequence of iterates $\{x_k\}$ of the form

$$x_{k+1} = \eta_{\tau h}(x_k - h\nabla f(x_k)). \quad (1.3)$$

*Escuela Politécnica Superior Universidad Carlos III de Madrid, Spain; moscoso@math.uc3m.es

†Department of Mathematics, Pennsylvania State University, USA; anovikov@math.psu.edu

‡Department of Mathematics, Stanford University, USA; papanicolaou@stanford.edu

§Department of Mathematics, Stanford University, USA; ryzhik@math.stanford.edu

Here, h is the step size,

$$\eta_a(x) = \begin{cases} x - a, & \text{if } x > a, \\ 0, & \text{if } -a < x < a, \\ x + a, & \text{if } x < -a \end{cases} \quad (1.4)$$

is the shrinkage-thresholding operator, and $\nabla f(x_k)$ denotes the gradient of $f(x) = \frac{1}{2}\|y - Ax\|^2$ at the current iterate x_k . Thus, $\nabla f(x_k) = A^*(Ax_k - y)$, where A^* denotes the complex conjugate transpose of A . The algorithm (1.3) involves only simple matrix-vector multiplications followed by a shrinkage-thresholding step.

For a fixed value of τ the solution to (1.2) differs in general from the solution of (1.1). In other words, exact recovery from noiseless data is not achieved by solving (1.2), unless the regularization parameter τ is sent to zero. However, it is well known that the convergence of (1.3) is slow for small values of the parameter τ . This issue is considered in detail in [5]. Variants of (1.3) have been proposed to speed up its convergence rate. In [2], for example, a fast version of ISTA is proposed (FISTA, described in more detail below in Section 3) that has as easy an implementation as (1.3) but has a much better convergence rate.

In this paper, we present an ordinary differential equations (ODE) approach to an iterative shrinkage-thresholding algorithm for solving ℓ_1 -minimization problems independently of the regularization parameter τ . We use a generalized Lagrange multiplier, or augmented Lagrangian, approach [3, 27, 29, 38, 40] to the relaxed problem (1.2) to impose exact recovery of the solution to (1.1). The exact solution is sought through an efficient algorithm obtained from a min-max variational principle, which is a special case of the Arrow-Hurwitz-Uzawa algorithm [1]. We prove that this algorithm yields the exact solution for all values of the parameter τ . Our only assumption is that the matrix A has full rank. The connection of the ODE method to the iterative shrinkage algorithm is provided by the Crandall-Liggett theory [15], which analyzes the convergence of an implicit finite difference discretization of the ODE. The theory works for infinite dimensional, monotone nonlinear problems as well. The performance of the algorithm, with and without noise in the data, is explored through several numerical simulations of array imaging problems.

The min-max variational principle used here is also behind the Bregman and linearized Bregman iterative algorithms [28, 37, 47, 48]. The fully implicit version of the algorithm is also analyzed in detail in [13, 23] using different techniques. Many other methods have been proposed in the literature to solve (1.1) and (1.2) with large data. We just mention here some of them: homotopy [22, 36, 44], interior-point methods [46], gradient projection [26], and proximal gradient in combination with iterative shrinkage-thresholding [2, 34, 35]. A detailed discussion and analysis of monotone operator splitting methods can be found in [39].

Finding the constrained, minimal l_1 norm solution in (1.1) does not imply that this solution vector has minimal support, even though the l_1 norm is sparsity promoting. Nevertheless in many applications, in imaging in particular, this optimization method does produce the minimal support, or minimal l_0 norm solution. The theory of compressed sensing [6–9, 20, 21, 45] gives conditions under which constrained l_1 and l_0 minimizations are equivalent. We do not address this issue here.

The paper is organized as follows. In Section 2 we motivate our approach, summarize our main results, and describe the numerical algorithm. Theorems 2.6 and 2.4 are the main results of this paper. A key ingredient in the proof of these theorems is Theorem 2.7 proved in Section 4. The proof of the variational principle of Theorem 2.2 is presented in Section 6. This result is originally due to [40] but we present it here for the convenience of the reader. In Section 3 we show the performance of the algorithm with and without noise in the data using some numerical experiments of array imaging. Finally, Section 7 contains conclusions.

Acknowledgment. MM was supported by the Spanish Ministry of Education and Science

grant FIS2010-18473, AN was supported by NSF grant DMS-0908011, LR was supported by AFOSR NSSEFF fellowship, and NSF grant DMS-0908507, and GP by AFOSR grant FA9550-11-1-0266. We thank Laurent Demanet for an interesting discussion, Alberto Bressan for bringing reference [15] to our attention, and Jalal Fadili for taking time to explain the literature on Arrow-Hurwicz-Uzawa algorithm, and pointing out the paper [13] to us.

2 Formulation and main results

We consider the constrained optimization problem (1.1) under the assumptions that (1.1) has a unique minimizer \bar{x} , and that A has full rank: the matrix AA^* is invertible.

2.1 The min-max variational principle

In order to find the minimizer \bar{x} , we recall the variational formulation of the l_1 -minimization problem [3, 29, 38, 40]. Define the function

$$F(x, z) = \tau \|x\|_{l_1} + \frac{1}{2} \|Ax - y\|^2 + \langle z, y - Ax \rangle,$$

for $x \in \mathbb{R}^n$ and $z \in \mathbb{R}^m$, and set

$$\bar{F} = \max_z \min_x \{F(x, z)\}. \quad (2.1)$$

Proposition 2.1 *The problem (2.1) has a solution, that is $-\infty < \bar{F} < +\infty$, and the max-min is attained.*

Proof. The function $F(x, z)$ is convex in x , and $\lim_{x \rightarrow \infty} F(x, z) = +\infty$, for any fixed z . Thus, $F(x, z)$ attains its minimum for a fixed z . Let us denote

$$l(x) = \tau \|x\|_{l_1} + \frac{1}{2} \|Ax - y\|^2, \quad (2.2)$$

and

$$h(z) = \min_x F(x, z) = \min_x [l(x) + \langle z, y - Ax \rangle]. \quad (2.3)$$

As the function $l(x)$ is convex, and $l(x) \rightarrow +\infty$, as $|x| \rightarrow \infty$, it follows that h is concave, as a minimum of affine functions, and $h(z) \rightarrow -\infty$, as $|z| \rightarrow \infty$. Thus, it attains its maximum $\max_z h(z)$. \square

In order to motivate the functional (2.1) we look at another natural way to impose the constraint in (1.1) by using a Lagrange multiplier. If we consider a functional

$$\tau \|x\|_{l_1} + \langle z, y - Ax \rangle, \quad (2.4)$$

then (at least, formally) its Euler-Lagrange equations for the extremum give us the *sub-differential* optimality condition

$$[A^*z]_i = \begin{cases} \tau, & \text{if } \bar{x}_i > 0, \\ -\tau, & \text{if } \bar{x}_i < 0, \end{cases} \quad \text{and } |[A^*z]_i| \leq \tau. \quad (2.5)$$

It is, however, difficult to work with (2.4), because if some of the entries of A^*z are larger than τ in absolute value, then (2.4) is not bounded from below as a function of x . Further, even if z is chosen according to the sub-differential condition (2.5), then the minimum may not be unique, even if A

is invertible. Indeed, consider a simple example: minimize $|x|$ subject to $x = 1$. Suppose $\tau = 1$, then (2.4) is $|x| + z(1 - x)$. Then $z = 1$ satisfies the sub-differential condition, and (2.4) becomes

$$|x| + (1 - x) = \begin{cases} 1, & \text{if } x > 0, \\ 1 - 2x, & \text{if } x < 0, \end{cases}$$

which has no minimum. The addition of a quadratic term to (2.4) regularizes this degeneracy. Since the function $l(x)$ in (2.2) is convex, (2.3) may be interpreted (up to a sign) as a generalized Legendre transform of $l(x)$.

The first observation is that if (1.1) has a unique minimum \bar{x} then the variational principle (2.1) finds \bar{x} exactly.

Theorem 2.2 *Assume that (1.1) has a unique minimum \bar{x} . Then we have*

$$\tau \|\bar{x}\|_{l_1} = \max_z \min_x F(x, z) \tag{2.6}$$

Moreover, we have $\tau \|\bar{x}\|_{l_1} = F(\bar{x}, z)$ for any z , and if $\min_x F(x, z) = \tau \|\bar{x}\|_{l_1}$ for some fixed z , then $\operatorname{argmin}_x F(x, z) = \bar{x}$.

This result can be found in [40] in a much greater generality. We present its proof below in the particular case we are interested in, for convenience of the reader.

It is remarkable that (2.6) holds for any value of $\tau > 0$ – this gives us a freedom to choose τ large or small, depending on a particular application. We also have the following well known result [40], which follows from the proof of Theorem 2.6 below.

Theorem 2.3 *Assume that (1.1) has a unique minimizer \bar{x} . Then, there exists a vector z such that $[A^*z]_i = \operatorname{sgn}(\bar{x}_i)$ if $\bar{x}_i \neq 0$, and $|[A^*z]_i| \leq 1$ if $\bar{x}_i = 0$.*

We say that z satisfies the sub-differential condition if there exists a minimizer of (1.1) such that

$$[A^*z]_i = \tau \operatorname{sgn}(\bar{x}_i) \text{ if } \bar{x}_i \neq 0, \text{ and } |[A^*z]_i| \leq \tau \text{ if } \bar{x}_i = 0. \tag{2.7}$$

We note that (2.7) is weaker than the sub-differential condition of [7] – there it is required that $|[A^*z]_i| < \tau$ if $\bar{x}_i = 0$, while we do not require the strict inequality. It follows from the proof of Theorem 2.3 that the exact extremum of $F(x, z)$ is achieved for any z that satisfies the sub-differential condition (2.7). Such z is not unique but, of course, our interest is not in finding z but in finding the minimizer of (1.1).

2.2 The ordinary differential equations method

In order to find \bar{x} , ideally, we would like to take the ODE point of view and generate a trajectory $(x(t), z(t))$ of the following system

$$\frac{dx}{dt} = -\nabla_x F(x, z), \quad \frac{dz}{dt} = \nabla_z F(x, z), \tag{2.8}$$

with the hope that $x(t) \rightarrow \bar{x}$ as $t \rightarrow +\infty$. There is an obvious degeneracy in the problem, namely, $F(\bar{x}, z) = \tau \|\bar{x}\|_{l_1}$ for all $z \in \mathbb{R}^m$. Hence, we can only hope to recover \bar{x} as there is no "optimal" z .

The obvious technical difficulty is that the function $F(x, z)$ is not differentiable in x at the points where $x_j = 0$ for some $j = 1, \dots, n$. Following [15], we interpret solutions of (2.8) as follows. Given $x \in \mathbb{R}^n$, let the sub-differential $\partial \|x\|_{l_1}$ be a subset of \mathbb{R}^n :

$$\partial \|x\|_{l_1} = \operatorname{sgn}(x_1) \times \dots \times \operatorname{sgn}(x_n).$$

Here $\text{sgn}(s)$, for $s \in \mathbb{R}$, is understood a subset of \mathbb{R} : $\text{sgn}(s) = \{1\}$ if $s > 0$, $\text{sgn}(s) = \{-1\}$ if $s < 0$ and $\text{sgn}(s) = [-1, 1]$ if $s = 0$. Then, instead of treating the system of ODEs (2.8) with a discontinuous right side, we consider

$$\begin{aligned} \frac{dx}{dt} - A^*(z - Ax + y) &\in -\tau \partial \|x\|_{l_1}, \\ \frac{dz}{dt} &= y - Ax, \end{aligned} \tag{2.9}$$

supplemented by the initial data $x(0) = x_0$, $z(0) = 0$. We say that $(x(t), z(t))$ is a strong solution to (2.9) on a time interval $0 \leq t \leq T$ if $x(t)$ and $z(t)$ are continuous, differentiable for almost all $t \in [0, T]$, $x(0) = x_0$, $z(0) = 0$, and (2.9) holds for almost all $t \in [0, T]$.

An important observation is that (2.9) is contractive, or, accretive in the sense of Crandall and Liggett [15]. That is, the following property holds: given any pair (x_1, z_1) , (x_2, z_2) and any $\xi_1 \in \partial \|x_1\|_{l_1}$, $\xi_2 \in \partial \|x_2\|_{l_1}$, we have:

$$\begin{aligned} &(A^*(z_1 - Ax_1) - \tau \xi_1 - A^*(z_2 - Ax_2) + \tau \xi_2) \cdot (x_1 - x_2) - (Ax_1 - Ax_2) \cdot (z_1 - z_2) \\ &= -\tau(\xi_1 - \xi_2) \cdot (x_1 - x_2) - \|A(x_1 - x_2)\|^2 \leq 0. \end{aligned} \tag{2.10}$$

The last inequality above follows from the component-wise monotonicity of the sub-differential $\partial \|x\|_{l_1}$. It follows from (2.10) and Theorems I and II of [15] that (2.9) has a unique strong solution. Our first result shows that this solution converges as $t \rightarrow +\infty$ to \bar{x} , the minimizer of (1.1).

Theorem 2.4 *Let (1.1) have a unique minimizer \bar{x} . Then, for any $\delta > 0$ there exists $T = T(\delta)$ such that the solution of (2.9) satisfies*

$$\|x(t) - \bar{x}\| < \delta, \text{ for all } t > T. \tag{2.11}$$

The time $T(\delta)$ depends only on δ , the initial data x_0 , and $\|AA^\|$ but not on the dimension n .*

2.3 The discrete algorithm

We consider the following numerical algorithm to solve (2.9):

$$\begin{aligned} \frac{x_{k+1} - x_k}{\Delta t} &= -\tau \xi_{k+1} + A^*(z_{k+1} + y - Ax_{k+1}), \\ \frac{z_{k+1} - z_k}{\Delta t} &= y - Ax_{k+1}, \end{aligned} \tag{2.12}$$

with the initial data $x_0 = x$, $z_0 = 0$. Here, ξ_{k+1} is a vector in the set $\partial \|x_{k+1}\|_{l_1}$.

A simple way to understand how (2.12) works is to consider the toy problem

$$\dot{r} = -\text{sgn}r. \tag{2.13}$$

An explicit discretization

$$\frac{r_{k+1} - r_k}{\Delta t} = -\xi_k,$$

with $\xi_k \in \text{sgn}(r_k)$, will start oscillating around $r = 0$ as soon as $r_k \in [-\Delta t, \Delta t]$, and will never converge to $x = 0$ for $\Delta t > 0$. On the other hand, the implicit discretization

$$\frac{r_{k+1} - r_k}{\Delta t} = -\xi_{k+1}, \tag{2.14}$$

with $\xi_{k+1} \in \text{sgn}(r_{k+1})$ behaves differently. If $r_k \in [-\Delta t, \Delta t]$, the implicit nature of this scheme shows that it is impossible to have $\xi_{k+1} = \pm 1$, which forces $\xi_{k+1} = r_k/\Delta t$ and $r_{k+1} = 0$. The implicit scheme is actually equivalent to soft thresholding:

$$r_{k+1} = \eta_{\Delta t}(r_k). \quad (2.15)$$

The function η_s here is defined by (1.4). This simple example already shows both the importance of using an implicit discretization, and that the implicit scheme has a simple explicit realization (2.15).

Theorems I and II of [15] not only provide existence of a strong solution to (2.9) but also show that it can be found by the implicit scheme (2.12).

Proposition 2.5 *Solution of (2.12) converges as $\Delta t \rightarrow 0$, uniformly on finite time intervals, to the unique strong solution of (2.9).*

Theorem 2.4 and Proposition 2.5 together imply immediately the following theorem.

Theorem 2.6 *Let the sequence x_n, z_n solve (2.12) with the initial data $x_0 = x, z_0 = 0$. Given any $\delta > 0$ there exists $h > 0$ and $T > 0$, so that for all $0 < \Delta t < h$ and all $k > [T/\Delta t]$ we have $|x_k - \bar{x}| < \delta$. The time T depends on δ , the initial data $x \in \mathbb{R}^n$, and the norm $\|AA^*\|$.*

If one examines the proof of Theorems I and II in [15], it is clear that the only term that should be discretized implicitly is $\text{sgn}x$ – the other terms can be discretized explicitly, keeping the statement of Proposition 2.5 intact. Hence, the result of Theorem 2.6 applies equally well to an Euler quazi-explicit modification of (2.12) that is easier to implement numerically:

$$\begin{aligned} x_{k+1} &= x_k - \xi_{k+1} + \Delta t A^*(z_k + y - Ax_k), \\ z_{k+1} &= z_k + \Delta t(y - Ax_k), \end{aligned} \quad (2.16)$$

where $\xi_{k+1} \in \tau \Delta t \partial \|x_{k+1}\|_{l_1}$ is a vector in the subdifferential of $\tau \Delta t \|x_{k+1}\|_{l_1}$. We call this scheme the generalized Lagrangian multiplier algorithm (GeLMA). As in the toy problem (2.13)-(2.15), it is equivalent to soft thresholding:

$$\begin{aligned} x_{k+1} &= \eta_{\tau \Delta t}(x_k + \Delta t A^*(z_k + y - Ax_k)), \\ z_{k+1} &= z_k + \Delta t(y - Ax_k). \end{aligned} \quad (2.17)$$

This scheme converges if $\Delta t < 1/\|A\|$ – that condition simply comes from the usual constraint for an explicit scheme for a linear system. GeLMA algorithm is extremely easy to implement numerically.

We also note that one can mimic the ODE proof of Theorem 2.4 directly on the numerical scheme, eliminating, in particular, the dependence of h on δ . Our objective, however, in part, is to explain the effectiveness of shrinking-thresholding algorithms in the language of differential equations, potentially opening the way for the application of other continuous techniques in such problems. Therefore, we have chosen to concentrate on the ODE proof.

2.3.1 The regularized ordinary differential equations

Since the system (2.9) has a "bad" right side, working with it directly is technically inconvenient. Hence, in order to prove Theorem 2.4, from which Theorem 2.6 follows, we consider a regularized system, introducing a single-valued approximation of $\text{sgn}x$:

$$G_\varepsilon(s) = \begin{cases} 1, & \text{if } s > \varepsilon, \\ s/\varepsilon, & \text{if } |s| < \varepsilon, \\ -1, & \text{if } s < -\varepsilon. \end{cases}$$

Here $\varepsilon > 0$ is a small regularization parameter that will be sent to zero at the end. With a slight abuse of notation, here, and in other instances when this should cause no confusion, we will also denote by $G_\varepsilon(x)$ a vector valued function with components $G_\varepsilon(x) = (G_\varepsilon(x_1), G_\varepsilon(x_2), \dots, G_\varepsilon(x_n))$. The regularized version of (2.9) is

$$\frac{dx_\varepsilon}{dt} = -\tau G_\varepsilon(x_\varepsilon) + A^*(z + y - Ax_\varepsilon), \quad \frac{dz_\varepsilon}{dt} = y - Ax_\varepsilon. \quad (2.18)$$

It has the same form (2.8), with $F(x, z)$ replaced by a differentiable approximation

$$F_\varepsilon(x, z) = \tau \sum_{j=1}^n r_\varepsilon(x_j) + f(x) + \langle z, y - Ax \rangle. \quad (2.19)$$

Here,

$$r_\varepsilon(s) = \begin{cases} |s|, & \text{if } s > \varepsilon, \\ s^2/(2\varepsilon) + \varepsilon/2, & \text{if } |s| < \varepsilon, \\ |s|, & \text{if } s < -\varepsilon, \end{cases}$$

is an approximation of $|s|$ known as the Huber function. We will denote below

$$\|x\|_{l_\varepsilon^1} = \sum_{j=1}^n r_\varepsilon(x_j), \quad (2.20)$$

though, of course, this is not a norm as it does not vanish at $x = 0$.

Theorem 2.7 *Let (1.1) have a unique minimizer \bar{x} . Then, for any $\delta > 0$ there exists $\varepsilon_0 = \varepsilon_0(\delta, n)$ and $T = T(\delta)$ such that for any ε , $0 < \varepsilon < \varepsilon_0$ the solution of (2.18) satisfies*

$$\|x_\varepsilon(t) - \bar{x}\| < \delta, \text{ for all } t > T. \quad (2.21)$$

The time $T(\delta)$ depends only on δ , the initial data x_0 , and $\|AA^\|$ but not on the dimension n .*

When the minimizer of (1.1) is not unique, the proof of Theorem 2.7 can be easily adapted to show that for any $\delta > 0$ there exists $\varepsilon_0(\delta)$ such that for any $\varepsilon \in (0, \varepsilon_0)$ and any limit point (as $t \rightarrow +\infty$) \bar{x}_ε of the trajectory $x_\varepsilon(t)$, we have $\|\bar{x}_\varepsilon - \bar{x}\| < \delta$ for some minimizer \bar{x} of (1.1).

Theorem 2.7 is the key ingredient in the proof of Theorem 2.6: together with a priori bounds on $x_\varepsilon(t)$ obtained in the course of its proof, they show that solution $x(t)$ of (2.9) is the limit of $x_\varepsilon(t)$ as $\varepsilon \rightarrow 0$, and thus it obeys the same bounds as $x_\varepsilon(t)$, finishing the proof.

3 Application to array imaging

In this section we illustrate the performance of our algorithm for array imaging of localized scatterers. The problem is to determine the location and reflectivities of small scatterers by sending a narrow band (single frequency) probing signal of wavelength λ from an active array and recording the backscattered field on this array [4]. In this paper we consider only single illumination by the central element of the array.

3.1 Array imaging in homogeneous media

The array has N transducers located at positions \mathbf{x}_p ($p = 1, \dots, N$) separated from each other by a given distance. In each numerical experiment there are M point-like scatterers of unknown reflectivities $\rho_j > 0$ located at unknown positions \mathbf{y}_{n_j} ($j = 1, \dots, M$). The scatterers are assumed to be within a bounded region at a distance L from the array, called the Image Window (IW). We discretize this IW with a uniform mesh of K points \mathbf{y}_j ($j = 1, \dots, K$), and assume that each scatterer is located at one of these K grid points, so $\{\mathbf{y}_{n_1}, \dots, \mathbf{y}_{n_M}\} \subset \{\mathbf{y}_1, \dots, \mathbf{y}_K\}$.

Furthermore, we assume that the medium between the array and the scatterers is homogeneous so wave propagation between any two points \mathbf{x} and \mathbf{y} is modeled by the free space Green function

$$\widehat{G}_0(\mathbf{y}, \mathbf{x}, \omega) = \frac{\exp(-i\kappa|\mathbf{x} - \mathbf{y}|)}{4\pi|\mathbf{x} - \mathbf{y}|}, \quad (3.1)$$

where $\kappa = \omega/c = 2\pi/\lambda$, and c is the reference wave speed in the medium. We also assume that the scatterers are well separated or are weak, so multiple scattering among them is negligible (this is the Born approximation). Under these conditions, the backscattered field measured at \mathbf{x}_r due to a pulse sent from \mathbf{x}_s , and reflected by the M scatterers in the IW, is given by

$$b_r(\omega) = \sum_{j=1}^M \rho_j \widehat{G}_0(\mathbf{x}_r, \mathbf{y}_{n_j}, \omega) \widehat{G}_0(\mathbf{y}_{n_j}, \mathbf{x}_s, \omega). \quad (3.2)$$

Next, we write the linear system that relates the reflectivity ρ_{0j} at each grid point \mathbf{y}_j of the IW ($j = 1, \dots, K$) and the data $b_r(\omega)$ measured at the array ($r = 1, \dots, N$). To this end, we introduce the *reflectivity vector* $\boldsymbol{\rho}_0 = (\rho_{01}, \rho_{02}, \dots, \rho_{0K})^T \in \mathbb{R}^K$ and the data vector $\mathbf{b}(\omega) = (b_1, b_2, \dots, b_N)^T \in \mathbb{R}^N$, where the superscript T means transpose. Thus, the image is a gridded array of K pixels, and the data is stacked into a vector of $N \ll K$ components. Furthermore, there are only a few scatterers in the IW so the vector $\boldsymbol{\rho}_0$ is sparse.

Let us consider the vector

$$\widehat{\mathbf{g}}_0(\mathbf{y}_j, \omega) = (\widehat{G}_0(\mathbf{x}_1, \mathbf{y}_j, \omega), \widehat{G}_0(\mathbf{x}_2, \mathbf{y}_j, \omega), \dots, \widehat{G}_0(\mathbf{x}_N, \mathbf{y}_j, \omega))^T,$$

that represents the signal at the array due to a point source at \mathbf{y}_j in the IW. Due to the spatial reciprocity $\widehat{G}_0(\mathbf{x}_i, \mathbf{y}, \omega) = \widehat{G}_0(\mathbf{y}, \mathbf{x}_i, \omega)$, it can also be interpreted as the illumination vector of the array at position \mathbf{y}_j . With this notation, we can write the linear system

$$A_\omega \boldsymbol{\rho}_0 = \mathbf{b}(\omega), \quad (3.3)$$

where A_ω is an $N \times K$ matrix whose j^{th} column is given by $\widehat{G}_0(\mathbf{y}_j, \mathbf{x}_s, \omega) \widehat{\mathbf{g}}_0(\mathbf{y}_j, \omega)$. Since $N \ll K$, (3.3) is an underdetermined linear system, and hence there can be many configurations of scatterers that match the data vector $\mathbf{b}(\omega)$. Array imaging is to solve (3.3) for $\boldsymbol{\rho}_0$.

A related problem to (3.3) has been studied in [10] in array imaging of localized scatterers from intensity-only measurements. Intensity measurements are interpreted as linear measurements of a rank one matrix associated with the unknown reflectivities. Since the rank minimization problem is NP-hard, it is replaced by the minimization of the nuclear norm of the decision matrix. This makes the problem convex and solvable in polynomial time. It is shown that exact recovery can be achieved by minimizing this problem.

3.2 Numerical Simulations

We consider here numerical experiments in 2D. Our linear array consists of 100 transducers that are one wavelength apart. Hence, the aperture of the array is $a = 100$. In each numerical experiment there are a few point-like scatterers of different reflectivity at a distance 120 from the array. The IW is discretized with 41×41 grid points. Hence, we have 1681 unknowns and 100 measurements. All the spatial units are expressed in units of the wavelength λ of the illuminating source.

Fig. 1 shows results from various scatterer's configurations with no noise in the data. In the top row we display the original scatterer's configurations and in the bottom row the corresponding images obtained by the ℓ_1 minimization GeLMA algorithm (2.17). These results show that this algorithm recovers the positions and reflectivities of the scatterers exactly when there is no noise in the data. To examine this issue more clearly we plot in Fig. 2 the vector solutions $\boldsymbol{\rho}$ (green crosses) and the exact vectors $\boldsymbol{\rho}_0$ (blue circles) for these three scatterer's configurations. There is not apparent difference between the exact and recovered solutions. Both, localization (support recovery) and strength estimation (reflectivities) are solved exactly in all the cases.

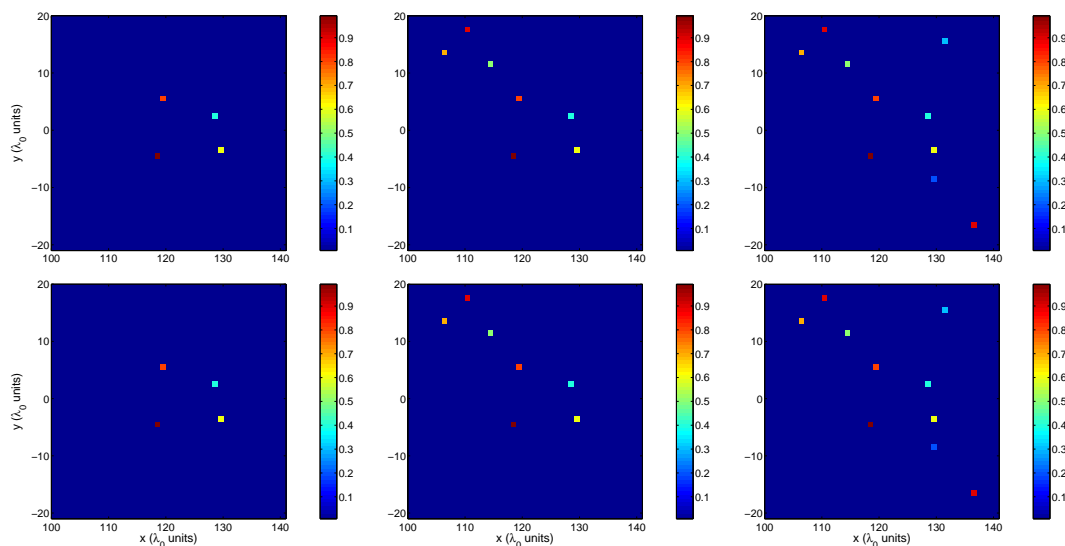


Figure 1: Top row: original configurations of the scatterers within the 41×41 IW. Bottom row: recovered images obtained by the ℓ_1 minimization GeLMA algorithm (2.17) with no noise in the data. $\tau = 20 \|A_\omega^T \mathbf{b}(\omega)\|_{l_\infty}$ and $N_{iter} = 300$.

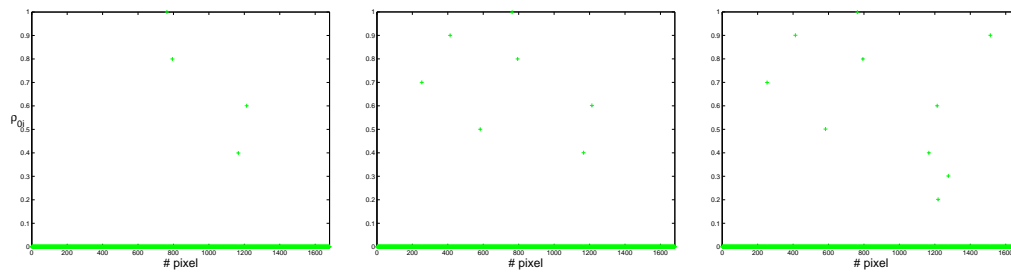


Figure 2: Comparison between the exact solutions (blue circles) and the solutions obtained with the GeLMA algorithm (green crosses) with no noise in the data.

An interesting feature of the GeLMA algorithm (2.17) is that it attains the exact solution of the basis pursuit problem for large values of the regularization parameter τ . This speeds up the convergence rate. Informally, this speed-up of convergence can be seen from the coercivity estimate (2.10) and the error estimate (4.7). Note that for other popular gradient based algorithms, such as ISTA or FISTA [2], τ has to be smaller than $\|A_\omega^T \mathbf{b}(\omega)\|_{l_\infty}$. Otherwise, they converge to the (maximally sparse) zero solution $\boldsymbol{\rho} = 0$. To examine this property in more detail, we show in Fig. 3 (left panel) plots of the ℓ_2 distance to the exact solution $\|\boldsymbol{\rho} - \boldsymbol{\rho}_0\|$ as function of the iteration number for various values of $\tau = \alpha \|A_\omega^T \mathbf{b}(\omega)\|_{l_\infty}$: $\alpha = 2$ (solid line), $\alpha = 5$ (dashed line), $\alpha = 10$ (dot-dashed line), and $\alpha = 20$ (dotted line). We observe that the larger the value of τ is, the faster is the convergence rate. Furthermore, for all the values of τ the algorithm achieves the exact solution $\boldsymbol{\rho}_0$.

In Fig. 3 (right panel) we compare the convergence rates of the GeLMA algorithm and the FISTA algorithm

$$\boldsymbol{\rho}^{(k)} = \eta_{\tau\alpha_k}(\boldsymbol{\rho}^{(k)} - \alpha_k \nabla f(\xi^{(k)})), \quad (3.4)$$

$$\alpha_{k+1} = \frac{1 + \sqrt{1 + 4\alpha_k^2}}{2}, \quad (3.5)$$

$$\xi^{(k+1)} = \boldsymbol{\rho}^{(k)} + \frac{\alpha_k - 1}{\alpha_{k+1}}(\boldsymbol{\rho}^{(k)} - \boldsymbol{\rho}^{(k-1)}), \quad (3.6)$$

for $\tau = 0.01 \|A_\omega^T \mathbf{b}(\omega)\|_{l_\infty}$. We choose a small value of τ because we are considering noise-free data in these examples. In (3.4)-(3.6), $\boldsymbol{\rho}_1$ and $\xi_2 = \boldsymbol{\rho}_1$ are given, and $\alpha_1 < 2/L$. We observe that the convergence rate of the FISTA algorithm (solid line) for $\tau = 0.01 \|A_\omega^T \mathbf{b}(\omega)\|_{l_\infty}$ is much slower than the convergence rate of the GeLMA algorithm for $\tau = 20 \|A_\omega^T \mathbf{b}(\omega)\|_{l_\infty}$. Even more, the FISTA algorithm with $\tau = 0.01 \|A_\omega^T \mathbf{b}(\omega)\|_{l_\infty}$ does not obtain the exact solution. To achieve the exact solution, we would have to let $\tau \rightarrow 0$.

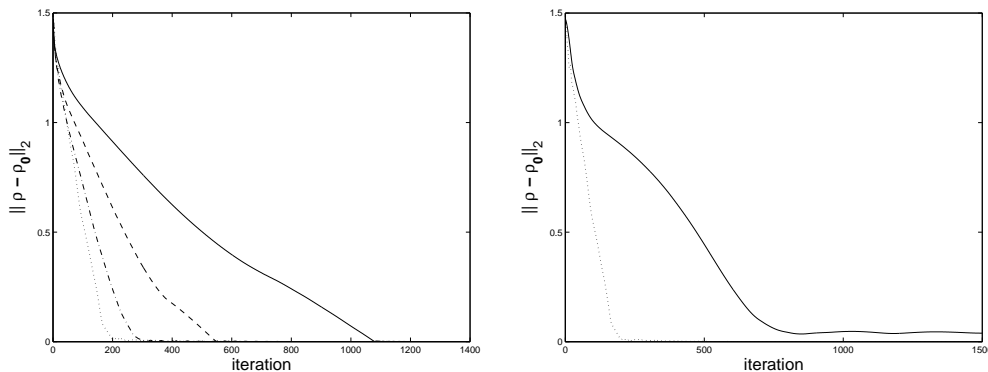


Figure 3: Right: Plots of the convergence rate of the GeLMA algorithm for various values of $\tau = \alpha \|A_\omega^T \mathbf{b}(\omega)\|_{l_\infty}$: $\alpha = 2$ (solid line), $\alpha = 5$ (dashed line), $\alpha = 10$ (dot-dashed line), and $\alpha = 20$ (dotted line). Left: Comparison of the converge rates of the GeLMA algorithm with $\alpha = 20$ (dotted line) and the FISTA method with $\alpha = 0.01$ (solid line). In these numerical experiments we have used the four scatterers configuration shown in the top right image of Fig. 1. Noiseless data.

Next, we examine the performance of the GeLMA algorithm under noise contaminated data $\mathbf{b}(\omega) + \mathbf{e}(\omega)$. The noise vector $\mathbf{e}(\omega)$ is generated by independent Gaussian random variables with zero mean and standard deviation $\beta \|\mathbf{b}(\omega)\|/\sqrt{N}$. Here, β is a parameter that measures the noise strength. In Fig. 4, we show the results for $\beta = 0.05$ (left column), $\beta = 0.1$ (middle column), and

$\beta = 0.3$ (right column). For a fixed step size Δt , the regularization parameter $\tau = \alpha \|A_\omega^T \mathbf{b}(\omega)\|_{l_\infty}$ controls the sparsity of the solution. Hence, one expects the algorithm to be more stable with respect to additive noise when τ is large. We plot in Fig. 4 the recovered images using different values of τ : $\alpha = 2$ (top row), $\alpha = 20$ (middle row) and $\alpha = 100$ (bottom row). We observe in the top row that the location of the scatterers is recovered exactly when there is 5% noise in the data (left plot). The recovered reflectivities are also quite close to the real ones. However, when the noise increases to 10% (middle plot) one scatterer is missing in the recovered image that also shows some ghost scatterers. As expected, the image gets worse when the noise is 30%, as can be seen in the right plot. The results are much better when we increase the value of α to 20 (middle row). With 5% noise in the data (left plot) both the location and reflectivities of the scatterers are very close to the real ones. Even with 10% noise in the data (middle plot) we can determine the location of the four scatterers. However, with 30% noise we miss the fourth scatterer. Finally, we show in the bottom row the recovered images using $\alpha = 200$. For 5% and 10% noise (left and middle images, respectively), the location of the scatterers is exact. Furthermore, the recovered reflectivities are very sharp. However, we still miss the location of one scatterer when there is 30% noise in the data, as can be seen in the right image of the bottom row of this figure. We plan to investigate in detail the robustness of the algorithm with respect to noise in a future publication.

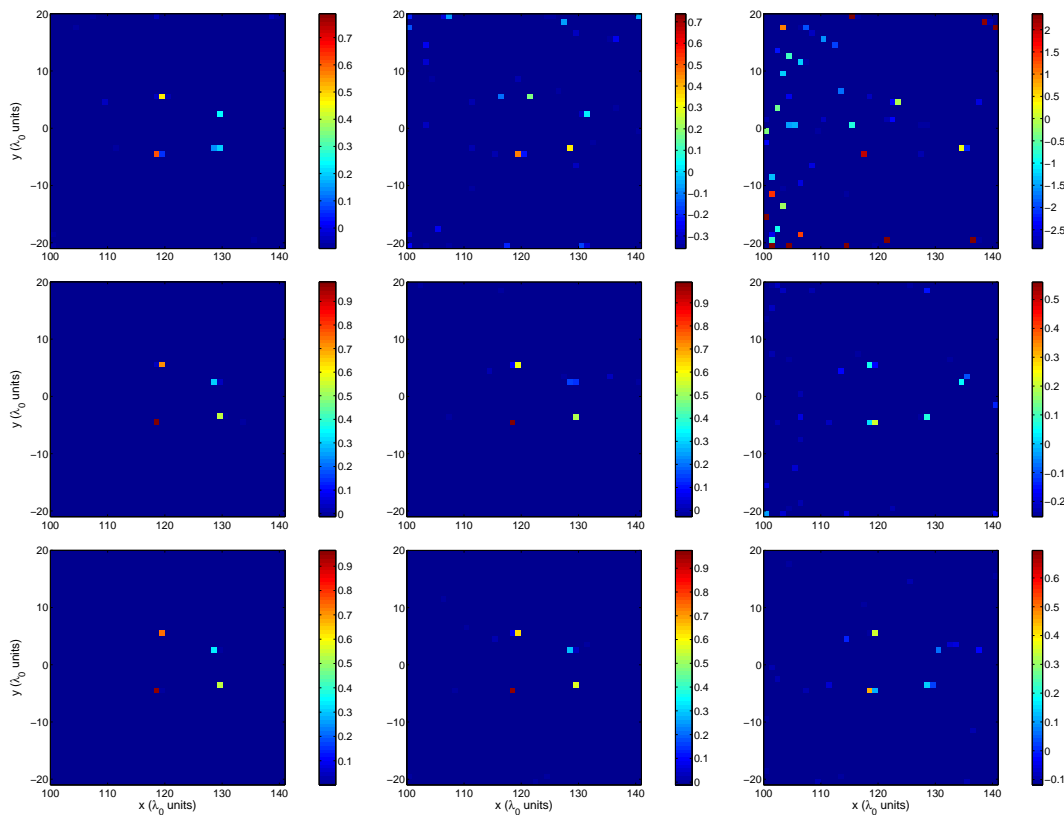


Figure 4: Impact of the regularization parameter $\tau = \alpha \|A_\omega^T \mathbf{b}(\omega)\|_{l_\infty}$ on the reconstructions for different amounts of noise in the data. Top row: Recovered images with $\alpha = 2$ and 5% noise (left), 10% noise (middle) and 30% noise (right). Middle row: same as top row but for $\alpha = 20$. Bottom row: same as top row but for $\alpha = 200$.

4 Proof of Theorems 2.4, 2.3 and 2.7

Theorems 2.4 and 2.3 are easy consequences of Theorem 2.7 and its proof.

4.1 Outline of the proof of Theorem 2.7

Let \bar{x} be the unique minimizer of (1.1) We write $x_\varepsilon = \bar{x} + q_\varepsilon$ and obtain

$$\frac{dq_\varepsilon}{dt} = -\tau G_\varepsilon(\bar{x} + q_\varepsilon) + A^*(z_\varepsilon - Aq_\varepsilon), \quad \frac{dz_\varepsilon}{dt} = -Aq_\varepsilon. \quad (4.1)$$

Our goal is now to show that $q_\varepsilon(t) \rightarrow 0$ as $t \rightarrow +\infty$. If we take the time-derivative of the first equation in (4.1), and use the second equation, we obtain:

$$\ddot{q}_\varepsilon + A^*A(\dot{q}_\varepsilon + q_\varepsilon) = -\tau g^\varepsilon(\bar{x} + q_\varepsilon)\dot{q}_\varepsilon. \quad (4.2)$$

Here $g^\varepsilon(x)$ is a diagonal matrix with the entries on the main diagonal given by

$$g_{ii}^\varepsilon(x) = \begin{cases} 0, & \text{if } |x_i| > \varepsilon, \\ 1/\varepsilon, & \text{if } |x_i| < \varepsilon. \end{cases} \quad (4.3)$$

Note that (4.2) is simply an equation for an oscillator with friction, and a forcing term in the right side. As the matrix A^*A is singular, the oscillator is degenerate. Therefore, it is reasonable to expect that the friction term $A^*A\dot{q}_\varepsilon$ in (4.2) by itself would ensure that $Aq_\varepsilon(t) \rightarrow 0$ as $t \rightarrow +\infty$, provided that the forcing does not interfere. However, the friction alone can not send $q_\varepsilon(t)$ to zero since it is degenerate. Moreover, in showing that $q_\varepsilon(t)$ becomes small as $t \rightarrow +\infty$, one has to use the fact that \bar{x} is the minimizer of (1.1) and not just any solution of $Ax = y$. The strategy of the proof is (i) to establish uniform bounds on $q_\varepsilon(t)$ and $z_\varepsilon(t)$, and (ii) show that any limit point of $q_\varepsilon(t)$ as $t \rightarrow +\infty$ is close to zero.

The a priori bounds are obtained in several steps. We first describe the required intermediate lemmas, and present their proofs later. The first step in the proof is the following lemma that provides a Lyapunov function for (4.1) and establishes a bound on $\|Aq_\varepsilon(t)\|$.

Lemma 4.1 *There exists a constant $C_0 > 0$ that is independent of ε (and depends only on the initial data x_0) so that*

$$\|\dot{q}_\varepsilon(t)\|^2 + \|Aq_\varepsilon(t)\|^2 + \int_0^\infty \|A\dot{q}_\varepsilon(s)\|^2 ds < C_0, \quad (4.4)$$

for all $\varepsilon < \varepsilon_0$ and for all $t > 0$.

The bound on $\|A\dot{q}_\varepsilon\|$ in Lemma 4.1 leads to a uniform bound on $z_\varepsilon(t)$.

Lemma 4.2 *There exists a constant $C > 0$ that is independent of $\varepsilon > 0$ so that $\|z_\varepsilon(t)\| \leq C$ for all $t > 0$.*

The next step is to show that $Aq_\varepsilon(t)$ is small for large times. Since $\dot{z}_\varepsilon = Aq_\varepsilon$, it follows from Lemma 4.2 that

$$\int_{t_1}^{t_2} Aq_\varepsilon(s) ds$$

is uniformly bounded for all $t_{1,2} > 0$. Together with the integral bound on $A\dot{q}_\varepsilon(t)$ in Lemma 4.1, this shows that $Aq_\varepsilon(t)$ becomes small at some "not too large" time.

Lemma 4.3 *There exists two constants $C_{1,2} > 0$ that are independent of $\varepsilon \in (0, \varepsilon_0)$ so that for any $k \in \mathbb{N}$ there exists a time $t_k < C_1 k^3$ such that for all $t \in (t_k, t_k + C_2 k)$ we have $\|Aq_\varepsilon(t)\| \leq C_1/k$ for all $\varepsilon < \varepsilon_0$.*

Next, using the bounds in Lemmas 4.1 and 4.2, as well as the precise form of the forcing term in (4.2), we obtain a uniform bound for $\|q_\varepsilon(t)\|$:

Lemma 4.4 *There exists a constant $C > 0$ so that we have*

$$\|\bar{x} + q_\varepsilon(t)\| \leq C, \quad (4.5)$$

for all $t > 0$ and all $\varepsilon > 0$.

The bound on $\|q_\varepsilon(t)\|$ allows us to strengthen Lemma 4.3 to include a bound on $\dot{q}_\varepsilon(t)$ "at some times" as well.

Lemma 4.5 *There exists a constant $C > 0$ that is independent of $\varepsilon \in (0, \varepsilon_0)$ so that for any $k \in \mathbb{N}$ there exists a time $s_k < Ck^3$ such that $\|Aq_\varepsilon(s_k)\|^2 + \|\dot{q}_\varepsilon(s_k)\|^2 \leq C/k$ for all $\varepsilon < \varepsilon_0$.*

The Lyapunov function in Lemma 4.1 and Lemma 4.5 together imply that $\dot{q}_\varepsilon(t)$ and $\dot{z}_\varepsilon(t)$ are not only "small sometimes" but rather tend to zero as $t \rightarrow +\infty$

Corollary 4.6 *There exists a constant $C > 0$ that is independent of $\varepsilon \in (0, \varepsilon_0)$ so that for any $n \in \mathbb{N}$ there exists a time $s_n = s_n(\varepsilon) < Cn^3$ such that $\|Aq_\varepsilon(s)\|^2 + \|\dot{q}_\varepsilon(s)\|^2 \leq C/n$ for all $\varepsilon < \varepsilon_0$ and all $s > s_n$.*

Corollary 4.6 shows that the right side of the ODE system (4.1) is small as $t \rightarrow +\infty$. The final step in the proof is to show that this implies that $q_\varepsilon(t)$ is small, and it is here that the condition that \bar{x} is the minimizer of (1.1) comes into play.

4.2 The end of the proof of Theorem 2.7

It follows from Corollary 4.6 that for any $\delta_0 > 0$ there exist $T = T(\delta_0)$, and $\varepsilon_0 = \varepsilon_0(\delta_0)$

$$\|A^* z_\varepsilon(t) - \tau G_\varepsilon(\bar{x} + q_\varepsilon(t))\| \leq \delta_0, \|Aq_\varepsilon(t)\| \leq \delta_0 \quad (4.6)$$

for all $\varepsilon \leq \varepsilon_0$ and $t > T$. The first inequality in (4.6) implies

$$|(A^* z_\varepsilon(t) - \tau G_\varepsilon(\bar{x} + q_\varepsilon(t)) \cdot (\bar{x} + q_\varepsilon(t))| \leq \delta_0 \|\bar{x} + q_\varepsilon(t)\|.$$

Using the second inequality from (4.6) in

$$|A^* z_\varepsilon(t) \cdot (\bar{x} + q_\varepsilon(t)) - A^* z_\varepsilon(t) \cdot \bar{x}| \leq \delta_0 \|z_\varepsilon(t)\|,$$

and denoting¹

$$\aleph_\varepsilon(x) = \sum_i x_i G_\varepsilon(x_i),$$

we obtain

$$|\tau \aleph(\bar{x} + q_\varepsilon(t)) - A^* z_\varepsilon(t) \cdot \bar{x}| \leq \delta_0 (\|z_\varepsilon(t)\| + \|\bar{x} + q_\varepsilon(t)\|).$$

¹The quantity $\aleph_\varepsilon(x)$ plays essentially the same role as $\|x\|_{l_1^\varepsilon}$ defined in (2.20). They are, however, quantitatively slightly different.

It also follows from the first inequality in (4.6) that

$$\|A^* z_\varepsilon(t)\|_{l_\infty} \leq \tau + \delta_0,$$

and thus

$$|(A^* z_\varepsilon(t) \cdot \bar{x})| \leq (\tau + \delta_0) \|\bar{x}\|_{l_1}.$$

As a consequence,

$$\mathfrak{N}(\bar{x} + q_\varepsilon(t)) - \|\bar{x}\|_{l_1} \leq \frac{\delta_0}{\tau} (\|\bar{x}\|_{l_1} + \|z_\varepsilon(t)\| + \|\bar{x} + q_\varepsilon(t)\|).$$

and therefore

$$\|\bar{x} + q_\varepsilon(t)\|_{l_1} - \|\bar{x}\|_{l_1} \leq \frac{\delta_0}{\tau} (\|\bar{x}\|_{l_1} + \|z_\varepsilon(t)\| + \|\bar{x} + q_\varepsilon(t)\|) + \varepsilon_0 n. \quad (4.7)$$

Here n is the dimension of q_ε . As \bar{x} is the unique minimizer, for any δ we can choose α and δ_0 sufficiently small so that estimates

$$\|\bar{x} + q_\varepsilon(t)\|_{l_1} - \|\bar{x}\|_{l_1} \leq \alpha, \quad \|Aq_\varepsilon(t)\| \leq \delta_0$$

imply that $\|q_\varepsilon\| < \delta$. Hence it remains to use uniform boundedness of $\bar{x} + q_\varepsilon(t)$ and $z_\varepsilon(t)$ and choose δ_0 and ε_0 so that

$$\frac{\delta_0}{\tau} (\|\bar{x}\|_{l_1} + \|z_\varepsilon(t)\| + \|\bar{x} + q_\varepsilon(t)\|) + \varepsilon_0 n \leq \alpha.$$

This finishes the proof of Theorem 2.7 except for the proof of Lemmas 4.1-4.5 and Corollary 4.6. \square

4.3 Proof of Theorem 2.4

Fix T_δ such that $|q_\varepsilon(t)| < \delta$ for all $T > T_\delta$. We know from the Arzela-Ascoli theorem that $q_\varepsilon(t) \rightarrow q(t)$ and $z_\varepsilon \rightarrow z(t)$ uniformly on $[0, T_\delta]$, after extracting a subsequence, and the functions $q(t)$ and $z(t)$ are Lipschitz on $[0, T_\delta]$, with the Lipschitz constant independent of $\delta > 0$. The second equation in (4.1), and the dominated convergence theorem imply that

$$z(t) = - \int_0^t Aq(s) ds, \quad (4.8)$$

whence

$$\dot{z} = -Aq, \quad z(0) = 0. \quad (4.9)$$

The family $f_\varepsilon(t) = G_\varepsilon(\bar{x} + q_\varepsilon(t))$ is uniformly bounded in $L^2[0, T_\delta]$. Hence, after possibly extracting a subsequence, it converges weakly in $L^2[0, T_\delta]$ to a limit $f(s)$. The (vector-valued) function $f(s)$ satisfies the following properties: (i) $-1 \leq f_j(t) \leq 1$, for all $0 \leq t \leq T_\delta$, $1 \leq j \leq N$, and (ii) if $q_j(t) \neq -\bar{x}_j$ then $f_j(t) = \text{sgn}(\bar{x}_j + q_j)$. It follows that for any $0 \leq t_1 < t_2 \leq T_\delta$ we have

$$q(t_2) - q(t_1) = -\tau \int_{t_1}^{t_2} f(s) ds + \int_{t_1}^{t_2} A^*(z(s) - Aq(s)) ds. \quad (4.10)$$

The aforementioned properties of $f(t)$ imply that $x(t) = \bar{x} + q(t)$ is a strong solution of (2.9). Uniqueness of the strong solution [15] implies that the whole family $x_\varepsilon(t) = \bar{x} + q_\varepsilon(t)$, $z_\varepsilon(t)$ converges to the solution of (2.9). The conclusion of Theorem 2.4 now follows from Theorem 2.7. \square

4.4 Proof of Theorem 2.3

Theorem 2.7 implies that as $\varepsilon \rightarrow 0$ and $t \rightarrow \infty$, along a subsequence, we have $\bar{z}_{\varepsilon_k} \rightarrow \bar{z}$ and $\bar{q}_{\varepsilon_k} \rightarrow \bar{0}$. Then the first estimate in (4.6) implies that $\bar{\lambda} = \bar{z}/\tau$ satisfies

$$\begin{aligned} [A^*\bar{\lambda}]_j &= \text{sgn}\bar{x}_j, \text{ if } \bar{x}_j \neq 0. \\ -1 \leq [A^*\bar{\lambda}]_j &\leq 1, \text{ if } \bar{x}_j = 0. \end{aligned} \quad (4.11)$$

This completes the proof of Theorem 2.3. \square

5 Proofs of auxiliary lemmas for the proof of Theorem 2.7

5.1 Proof of Lemma 4.1

Multiplying (4.2) by $\dot{q}_\varepsilon(t)$, gives

$$\frac{1}{2} \frac{d}{dt} (\|\dot{q}_\varepsilon(t)\|^2 + \|Aq_\varepsilon(t)\|^2) = -\|A\dot{q}_\varepsilon(t)\|^2 - \tau \langle g^\varepsilon(\bar{x} + q_\varepsilon) \dot{q}_\varepsilon, \dot{q}_\varepsilon \rangle. \quad (5.1)$$

Let

$$N_t^\varepsilon = \int_0^t \langle g^\varepsilon(\bar{x} + q_\varepsilon(s)) \dot{q}_\varepsilon(s), \dot{q}_\varepsilon(s) \rangle ds = \sum_{j=1}^n \int_0^t g_{jj}^\varepsilon(\bar{x}_j + q_{\varepsilon,j}(s)) |\dot{q}_{\varepsilon,j}(s)|^2 ds \geq 0, \quad (5.2)$$

then integrating (5.1) in time we get

$$\frac{1}{2} (\|\dot{q}_\varepsilon(0)\|^2 + \|Aq_\varepsilon(0)\|^2) = \frac{1}{2} (\|\dot{q}_\varepsilon(T)\|^2 + \|Aq_\varepsilon(T)\|^2) + \tau N_T^\varepsilon + \int_0^T \|A\dot{q}_\varepsilon\|^2 dt, \quad (5.3)$$

and (4.4) follows. Note that $\|\dot{q}_\varepsilon(0)\|$ is uniformly bounded in $\varepsilon > 0$ since the function $G_\varepsilon(s)$ takes values in the interval $[-1, 1]$. \square

5.2 Proof of Lemma 4.2

Differentiating the second equation in (4.1) we obtain

$$\ddot{z}_\varepsilon + AA^*(\dot{z}_\varepsilon + z_\varepsilon) = \tau AG_\varepsilon(\bar{x} + q_\varepsilon(t)). \quad (5.4)$$

Let us multiply this equation by e^t and integrate, to obtain

$$\int_0^t e^s \ddot{z}_\varepsilon(s) ds + e^t AA^* z_\varepsilon(t) = \tau A \int_0^t e^s G_\varepsilon(\bar{x} + q_\varepsilon(s)) ds, \quad (5.5)$$

since $z(0) = 0$. We estimate, using (4.4):

$$\left\| \int_0^t e^t \ddot{z}_\varepsilon(s) ds \right\| \leq \left(\int_0^t e^{2t} ds \int_0^t \|\ddot{z}_\varepsilon(s)\|^2 ds \right)^{1/2} \leq C e^t \left(\int_0^t \|A\dot{q}_\varepsilon(s)\|^2 ds \right)^{1/2} \leq C e^t.$$

As $|G_{\varepsilon,j}| \leq 1$ for all $1 \leq j \leq n$, we also have

$$\left\| A \int_0^t e^s G_\varepsilon(\bar{x} + q_\varepsilon(s)) ds \right\| \leq C e^t.$$

Since the matrix AA^* is invertible, we obtain from (5.5) that $\|z_\varepsilon(t)\| \leq C$. \square

5.3 Proof of Lemma 4.3

Let us set $y_\varepsilon(t) = Aq_\varepsilon(t)$. As $z_\varepsilon(t)$ is uniformly bounded, there exists a constant $C > 0$ that is independent of ε so that

$$\int_{t_1}^{t_2} y_\varepsilon(s) ds < C, \quad (5.6)$$

for all $0 < t_1 < t_2$. If we take an integer $n = Ck$, we have

$$\left\| \frac{1}{n} \int_t^{t+n} y_\varepsilon(s) ds \right\| < \frac{1}{2k}, \quad (5.7)$$

for all $t > 0$, and

$$\|y_\varepsilon(t)\| \leq \left\| \frac{1}{n} \int_t^{t+n} y_\varepsilon(s) ds \right\| + \frac{1}{n} \int_t^{t+n} \sqrt{s-t} \left(\int_t^s \|\dot{y}_\varepsilon(\xi)\|^2 d\xi \right)^{1/2} ds \leq \frac{1}{2k} + \sqrt{n} \left(\int_t^{t+n} \|\dot{y}_\varepsilon(s)\|^2 ds \right)^{1/2}. \quad (5.8)$$

Lemma 4.1 implies that given n there exist at most $Ck^2n = Ck^3$ integers l such that

$$\int_l^{l+2n} \|\dot{y}_\varepsilon(s)\|^2 ds > \frac{1}{4k^2n}.$$

It follows that there exists $k_0 < Ck^3$ such that

$$\int_{k_0}^{k_0+2n} \|\dot{y}_\varepsilon(s)\|^2 ds < \frac{1}{4k^2n}.$$

Then, for all $t \in (k_0, k_0 + n)$ we have

$$\int_t^{t+n} \|\dot{y}_\varepsilon(s)\|^2 ds < \frac{1}{4k^2n},$$

whence

$$\|y_\varepsilon(t)\| \leq \frac{C}{k}, \quad (5.9)$$

for all $t \in (k_0, k_0 + n)$. \square

5.4 Proof of Lemma 4.4

Let us recall (4.2):

$$\ddot{q}_\varepsilon + A^*A(\dot{q}_\varepsilon + q_\varepsilon) = -\tau g^\varepsilon(\bar{x} + q_\varepsilon) \dot{q}_\varepsilon, \quad (5.10)$$

Multiply this equation by q_ε and integrate:

$$\begin{aligned} & \langle q_\varepsilon(t), \dot{q}_\varepsilon(t) \rangle - \langle q_\varepsilon(0), \dot{q}_\varepsilon(0) \rangle + \frac{1}{2} \|Aq_\varepsilon(t)\|^2 - \frac{1}{2} \|Aq_\varepsilon(0)\|^2 + \int_0^t \|Aq_\varepsilon(s)\|^2 ds \\ &= \int_0^t \|\dot{q}_\varepsilon(s)\|^2 ds - \tau \int_0^t \langle g^\varepsilon(\bar{x} + q_\varepsilon) \dot{q}_\varepsilon, q_\varepsilon \rangle ds \end{aligned} \quad (5.11)$$

Next, set

$$v_\varepsilon(t) = - \int_0^t q_\varepsilon(s) ds,$$

so that $z_\varepsilon(t) = Av_\varepsilon(t)$, and $v_\varepsilon(0) = 0$. We rewrite (4.1) as

$$\frac{dq_\varepsilon}{dt} = -\tau G_\varepsilon(\bar{x} + q_\varepsilon) + A^*A(v_\varepsilon - q_\varepsilon), \quad \frac{dv_\varepsilon}{dt} = -q_\varepsilon. \quad (5.12)$$

Consider the function

$$Q(t) = \frac{1}{2}\|A(v_\varepsilon(t) - q_\varepsilon(t))\|^2 + \tau\|\bar{x} + q_\varepsilon(t)\|_{l_\varepsilon^1}. \quad (5.13)$$

Then we have

$$\begin{aligned} \frac{dQ}{dt} &= \tau\langle G_\varepsilon(\bar{x} + q_\varepsilon), \dot{q}_\varepsilon \rangle - \langle A^*A(v_\varepsilon - q_\varepsilon), \dot{q}_\varepsilon \rangle + \langle A^*A(v_\varepsilon - q_\varepsilon), \dot{v}_\varepsilon \rangle \\ &= -\|\dot{q}_\varepsilon\|^2 + \frac{1}{2}\frac{d}{dt}\|Av_\varepsilon\|^2 - \langle Av_\varepsilon, Aq_\varepsilon \rangle = -\|\dot{q}_\varepsilon\|^2 + \frac{1}{2}\frac{d}{dt}\|z_\varepsilon\|^2 + \|\dot{z}_\varepsilon\|^2. \end{aligned} \quad (5.14)$$

As $z_\varepsilon(0) = 0$, it follows that

$$\begin{aligned} &\|A(v_\varepsilon(t) - q_\varepsilon(t))\|^2 + \tau\|\bar{x} + q_\varepsilon(t)\|_{l_\varepsilon^1} - \|A(v_\varepsilon(0) - q_\varepsilon(0))\|^2 - \tau\|\bar{x} + q_\varepsilon(0)\|_{l_\varepsilon^1} \\ &= \frac{\|z_\varepsilon(t)\|^2}{2} - \int_0^t \|\dot{q}_\varepsilon(s)\|^2 ds + \int_0^t \|\dot{z}_\varepsilon(s)\|^2 ds. \end{aligned}$$

This can be re-written as

$$\|z_\varepsilon(t) - Aq_\varepsilon(t)\|^2 + \tau\|\bar{x} + q_\varepsilon(t)\|_{l_\varepsilon^1} + \int_0^t \|\dot{q}_\varepsilon(s)\|^2 ds = \frac{\|z_\varepsilon(t)\|^2}{2} + \int_0^t \|Aq_\varepsilon(s)\|^2 ds + C_0. \quad (5.15)$$

Adding (5.11) and (5.15) gives:

$$\begin{aligned} &\langle q_\varepsilon(t), \dot{q}_\varepsilon(t) \rangle + \frac{1}{2}\|Aq_\varepsilon(t)\|^2 + \|z_\varepsilon(t) - Aq_\varepsilon(t)\|^2 + \tau\|\bar{x} + q_\varepsilon(t)\|_{l_\varepsilon^1} + \\ &= -\tau \int_0^t \langle g^\varepsilon(\bar{x} + q_\varepsilon), \dot{q}_\varepsilon, q_\varepsilon \rangle ds + \frac{\|z_\varepsilon(t)\|^2}{2} + C'_0, \end{aligned} \quad (5.16)$$

with the constant C'_0 that only depends on the initial data. Lemmas 4.1 and 4.2 imply then

$$\langle q_\varepsilon(t), \dot{q}_\varepsilon(t) \rangle + \tau\|\bar{x} + q(t)\|_{l_\varepsilon^1} = -\tau \int_0^t \langle g^\varepsilon(\bar{x} + q_\varepsilon), \dot{q}_\varepsilon, q_\varepsilon \rangle ds + r(t), \quad (5.17)$$

with a uniformly bounded function $r(t)$: $|r(t)| \leq C$. We claim that there exists $C > 0$ that is independent of ε and t so that

$$\left| \int_0^t \langle g^\varepsilon(\bar{x} + q_\varepsilon), \dot{q}_\varepsilon, q_\varepsilon \rangle ds \right| \leq C. \quad (5.18)$$

Indeed, let us fix some $1 \leq j \leq n$ and look at

$$I = \int_0^t g_{jj}^\varepsilon(\bar{x} + q_\varepsilon(s)) q_{\varepsilon,j}(s) \dot{q}_{\varepsilon,j}(s) ds = \frac{1}{\varepsilon} \sum_{k=1}^Q \int_{s_k}^{s'_k} q_{\varepsilon,j}(s) \dot{q}_{\varepsilon,j}(s) ds = \frac{1}{2\varepsilon} \sum_{k=1}^Q (\|q_{\varepsilon,j}(s'_k)\|^2 - \|q_{\varepsilon,j}(s_k)\|^2). \quad (5.19)$$

Here (s_k, s'_k) , $k = 1, \dots, Q$, are the time intervals that $q_j(s)$ spends in the interval $(-\bar{x}_j - \varepsilon, -\bar{x}_j + \varepsilon)$, and $q_j(s_k) = \bar{x}_j \pm \varepsilon$, depending on whether q_j enters this interval from above or below, and similarly for $q_\varepsilon(s'_k)$. It is easy to see that $q_j(s'_k) = q_j(s_{k+1})$, whence (5.19) is a telescoping sum, giving

$$I = \frac{1}{2\varepsilon} (\|q_{\varepsilon,j}(s'_Q)\|^2 - \|q_{\varepsilon,j}(s_1)\|^2).$$

As both terms in the right side above can take only the values $-\bar{x}_j \pm \varepsilon$, we conclude that $|I| \leq C$, so that (5.18) holds. Now, (5.17) becomes

$$\langle q_\varepsilon(t), \dot{q}_\varepsilon(t) \rangle + \tau \|\bar{x} + q_\varepsilon(t)\|_{l_1^\varepsilon} \leq C. \quad (5.20)$$

As $\|x\| \leq \|x\|_{l_1}$, using the triangle inequality, we obtain the following inequality for $m_\varepsilon(t) = \|q_\varepsilon(t)\|$:

$$m_\varepsilon(t) \dot{m}_\varepsilon(t) + C_1 m_\varepsilon(t) \leq C_2.$$

Now, the comparison principle implies that $m_\varepsilon(t) \leq C'$ for all $t > 0$, and the proof of Lemma 4.4 is complete. \square

5.5 Proof of Lemma 4.5

Let us choose t_k and $t_{k'}$ as in the proof of Lemma 4.3. The estimate for $\|Aq_\varepsilon(t_k)\|$ is exactly as in that Lemma. Next, dividing (5.15) by $C_2 k = t'_k - t_k$ we get, due to the boundedness of $z_\varepsilon(t)$ and $q_\varepsilon(t)$:

$$\frac{1}{t'_k - t_k} \int_{t_k}^{t'_k} \|\dot{q}_\varepsilon(s)\|^2 ds \leq \frac{C}{k} + \frac{C}{k} \int_{t_k}^{t'_k} \|Aq_\varepsilon(s)\|^2 ds \leq \frac{C}{k} + \frac{C}{k^2}. \quad (5.21)$$

It follows that there exists a time $s_k \in (t_k, t'_k)$ such that $\|\dot{q}_\varepsilon(s_k)\| \leq C/\sqrt{k}$. \square

5.6 Proof of Corollary 4.6

This follows immediately from Lemma 4.5 and (5.1), as the latter implies that

$$\|\dot{q}_\varepsilon(t)\|^2 + \|Aq_\varepsilon(t)\|^2 \leq \|\dot{q}_\varepsilon(s_n)\|^2 + \|Aq_\varepsilon(s_n)\|^2 \leq \frac{C}{n}, \quad (5.22)$$

for all $t > s_n$. \square

6 The proof of Theorem 2.2

We will use Theorem 2.3 in order to prove Theorem 2.2. The role of the vector z that satisfies the sub-differential condition can be seen from the following lemma.

Lemma 6.1 *Suppose the sub-differential condition does not hold for a particular z . Then for this z we have a strict inequality*

$$h(z) = \min_x F(x, z) < \tau \|\bar{x}\|_{l_1}. \quad (6.1)$$

Proof. Assume that z does not satisfy the sub-differential condition, that is, either

- (i) $|[A^*z]_i| > \tau$ for some i , or
- (ii) $|[A^*z]_i| \leq \tau$, but $[A^*z]_i \neq \tau \text{sign}(\bar{x}_i)$ for some i such that $\bar{x}_i \neq 0$.

We will show that

$$F(\bar{x} + q, z) < F(\bar{x}, z) = \tau \|\bar{x}\|_{l_1}, \quad (6.2)$$

for some (sufficiently small) q , which implies (6.1). We will now construct q explicitly.

Assume first that (i) holds: $|[A^*z]_i| > \tau$ for some i . Then, set $r = [A^*\bar{z}]_i$, and choose q so that

$$q_k = \begin{cases} \varepsilon \operatorname{sign}(r), & \text{if } k = i, \\ 0, & \text{otherwise.} \end{cases}$$

We have

$$\begin{aligned} F(\bar{x} + q, z) &= \tau\|\bar{x} + q\|_{l_1} + \frac{1}{2}\|Aq\|^2 - \langle A^*z, q \rangle = \tau\|\bar{x}\|_{l_1} + \tau(|\bar{x}_i + \varepsilon \operatorname{sign}(r)| - |\bar{x}_i|) + \frac{1}{2}\|Aq\|^2 - \varepsilon|r| \\ &\leq \tau\|\bar{x}\|_{l_1} + \varepsilon\tau - \varepsilon|r| + \frac{1}{2}\|Aq\|^2 \leq \varepsilon\tau\|\bar{x}\|_{l_1} + \varepsilon\tau - \varepsilon|r| + C\varepsilon^2 < \tau\|\bar{x}\|_{l_1}, \end{aligned}$$

provided that we choose ε sufficiently small.

Similarly, if (ii) holds, pick some i such that $\bar{x}_i \neq 0$ but $[A^*z]_i \neq \tau \operatorname{sign}(\bar{x}_i)$. Assume first that $[A^*z]_i = r \operatorname{sign}(\bar{x}_i)$ with $0 < |r| < \tau$. Pick $\varepsilon \in (0, |\bar{x}_i|)$ and choose q with the components

$$q_k = \begin{cases} -\varepsilon \operatorname{sign}(\bar{x}_i), & \text{if } k = i, \\ 0, & \text{otherwise.} \end{cases} \quad (6.3)$$

The computation is similar:

$$\begin{aligned} F(\bar{x} + q, z) &= \tau\|\bar{x} + q\|_{l_1} + \frac{1}{2}\|Aq\|^2 - \langle A^*\bar{z}, q \rangle = \tau\|\bar{x}\|_{l_1} + \tau(|\bar{x}_i - \varepsilon \operatorname{sign}(\bar{x}_i)| - |\bar{x}_i|) \\ &\quad + \frac{1}{2}\|Aq\|^2 + \varepsilon r \leq \tau\|\bar{x}\|_{l_1} - \varepsilon\tau + \varepsilon r + \frac{1}{2}\|Aq\|^2 \leq \varepsilon\tau\|\bar{x}\|_{l_1} - \varepsilon\tau + \varepsilon r + C\varepsilon^2 < \tau\|\bar{x}\|_{l_1}, \end{aligned} \quad (6.4)$$

provided that ε is sufficiently small. The last case case to consider is when (ii) holds, but $[A^*z]_i = -\tau \operatorname{sign}(\bar{x}_i)$. We still choose q as in (6.3), and the computation is identical to (6.4), with $r = -\tau$. This completes the proof of Lemma 6.1. \square

Proof of Theorem 2.2. We trivially have

$$h(z) = \min_x F(x, z) \leq F(\bar{x}, z) = \tau\|\bar{x}\|_{l_1},$$

for all z . Thus, the conclusion of Theorem 2.2 would follow if we show that there exists \bar{z} such that $h(\bar{z}) = \tau\|\bar{x}\|_{l_1}$. That is, we need to show that for any $q \neq 0$ and some \bar{z} , we have

$$F(\bar{x} + q, \bar{z}) = \tau\|\bar{x} + q\|_{l_1} + \frac{1}{2}\|Aq\|^2 - \langle A^*\bar{z}, q \rangle > F(\bar{x}, \bar{z}) = \tau\|\bar{x}\|_{l_1}. \quad (6.5)$$

We claim that (6.5) is true for any \bar{z} that satisfies the sub-differential condition (2.7) – recall that Theorem 2.3 implies that such \bar{z} exists. Let \bar{z} satisfy the sub-differential condition (2.7):

$$[A^*\bar{z}]_i = \tau \operatorname{sign}\bar{x}_i, \text{ if } i \in S_1, \quad (6.6)$$

$$|[A^*\bar{z}]_i| \leq \tau, \text{ if } i \in S_0. \quad (6.7)$$

We denoted here by S_1 the set of indices i such that $\bar{x}_i \neq 0$, and by S_0 the set of indices i such that $\bar{x}_i = 0$.

The function $F(\bar{x} + q, \bar{z})$ is convex in q . Hence, it suffices to show that $q = 0$ is a strict local minimum, that is, show that (6.5) holds for q small enough. In particular, we may assume that

$$\operatorname{sign}(\bar{x}_i + q_i) = \operatorname{sign}(\bar{x}_i), \text{ if } i \in S_1. \quad (6.8)$$

Now, we obtain from (6.7):

$$\tau|q_i| - [A^* \bar{z}]_i q_i \geq 0, \quad i \in S_0, \quad (6.9)$$

while for $i \in S_1$, we use (6.8) and (6.6) to obtain

$$\tau|\bar{x}_i + q_i| - [A^* \bar{z}]_i q_i = \tau(\operatorname{sgn} \bar{x}_i)(\bar{x}_i + q_i) - \tau(\operatorname{sgn} \bar{x}_i)q_i = \tau(\operatorname{sgn} \bar{x}_i)\bar{x}_i = \tau|\bar{x}_i|, \quad i \in S_1. \quad (6.10)$$

We deduce from (6.9)-(6.10) that

$$\begin{aligned} F(\bar{x} + q, \bar{z}) &= \tau\|\bar{x} + q\|_{l_1} + \frac{1}{2}|Aq|^2 - \langle A^* \bar{z}, q \rangle = \sum_{i \in S_1} (\tau|\bar{x}_i + q_i| - [A^* \bar{z}]_i q_i) + \sum_{i \in S_0} (\tau|q_i| - [A^* \bar{z}]_i q_i) \\ &+ \frac{1}{2}|Aq|^2 \geq \sum_{i \in S_1} \tau|\bar{x}_i| + \frac{1}{2}|Aq|^2 = \tau\|\bar{x}\|_{l_1} + \frac{1}{2}|Aq|^2. \end{aligned} \quad (6.11)$$

Therefore, we have $F(\bar{x} + q, \bar{z}) > \tau\|x\|_{l_1}$ unless $Aq = 0$. However, if $Aq = 0$, then

$$F(\bar{x} + q, z) = \tau\|\bar{x} + q\|_{l_1} > \tau\|\bar{x}\|_{l_1},$$

because \bar{x} is the unique minimizer of (1.1). Therefore, (6.5) holds for all q . \square

7 Conclusions

We have shown using ordinary differential equation methods that the relaxed l_1 minimization algorithm for problems with underdetermined linear constraints converges independently of the regularization parameter. In the examples in array imaging the observed convergence rates are faster than the theory implies, which means that more analysis is needed. The algorithm is robust to noise although we have not shown this theoretically. Finally, as the convergence rates are independent of dimension, generalization to the infinite-dimensional case is straightforward.

References

- [1] Kenneth J. Arrow, Leonid Hurwicz, and Hirofumi Uzawa, *Studies in linear and non-linear programming*, With contributions by H. B. Chenery, S. M. Johnson, S. Karlin, T. Marschak, R. M. Solow. Stanford Mathematical Studies in the Social Sciences, vol. II, Stanford University Press, Stanford, Calif., 1958.
- [2] Amir Beck and Marc Teboulle, *A Fast Iterative Shrinkage-Thresholding Algorithm for Linear Inverse Problems*, SIAM J. Imag. Sci. **2** (2009), 183–202, DOI 10.1137/080716542.
- [3] Dimitri P. Bertsekas, *Convex optimization theory*, Athena Scientific, Nashua, NH, 2009.
- [4] Liliana Borcea, George Papanicolaou, Chrysoula Tsogka, and James Berryman, *Imaging and time reversal in random media*, Inverse Problems **18** (2002), no. 5, 1247.
- [5] Kristian Bredies and Dirk A. Lorenz, *Linear Convergence of Iterative Soft-Thresholding*, J Fourier Anal Appl **14** (2008), 813–837, DOI 10.1007/s00041-008-9041-1.
- [6] Emmanuel J. Candès and Terence Tao, *Decoding by linear programming*, IEEE Trans. Inform. Theory **51** (2005), no. 12, 4203–4215, DOI 10.1109/TIT.2005.858979. MR2243152 (2007b:94313)
- [7] ———, *Near optimal signal recovery from random projections: Universal encoding strategies*, IEEE Trans. Inform. Theory **52** (2006), no. 1, 5406–5425.
- [8] Emmanuel J. Candès and Justin Romberg, *Quantitative robust uncertainty principles and optimally sparse decompositions*, Foundations of Computational Mathematics **6** (2006), no. 1, 227254.
- [9] Emmanuel J. Candès, Justin Romberg, and Terence Tao, *Robust uncertainty principles: Exact signal reconstruction from highly incomplete frequency information*, IEEE Trans. Inform. Theory **52** (2006), no. 1, 489–509.
- [10] Anwei Chai, Miguel Moscoso, and George Papanicolaou, *Array imaging using intensity-only measurements*, Inverse Problems **27** (2011), no. 1, 015005.

- [11] ———, *Robust imaging of localized scatterers using the singular value decomposition and ℓ_1 minimization*, Preprint.
- [12] Antonin Chambolle, Ronald A. De Vore, Nam-Yong Lee, and Bradley J. Lucier, *Nonlinear wavelet image processing: variational problems, compression, and noise removal through wavelet shrinkage*, Image Processing, IEEE Transactions on **7** (1998), no. 3, 319–335, DOI 10.1109/83.661182.
- [13] Antonin Chambolle and Thomas Pock, *A first-order primal-dual algorithm for convex problems with applications to imaging*, J. Math. Imaging Vision **40** (2011), no. 1, 120–145.
- [14] Tony F. Chan and Jianhong Shen, *Image processing and analysis*, Society for Industrial and Applied Mathematics (SIAM), Philadelphia, PA, 2005. Variational, PDE, wavelet, and stochastic methods.
- [15] Michael G. Crandall and Thomas M. Liggett, *Generation of semi-groups of nonlinear transformations on general Banach spaces*, Amer. J. Math. **93** (1971), 265–298.
- [16] Ingrid Daubechies, Michel Defrise, and Christine De Mol, *An iterative thresholding algorithm for linear inverse problems with a sparsity constraint*, Comm. Pure Appl. Math. **57** (2004), no. 11, 1413–1457.
- [17] Christine De Mol and Michael Defrise, *A note on wavelet-based inversion algorithms*, Contemporary Mathematics **313** (2002), 85–96.
- [18] David Donoho, *De-noising by soft-thresholding*, Information Theory, IEEE Transactions on **41** (1995), no. 3, 613–627, DOI 10.1109/18.382009.
- [19] Scott S. Chen, David Donoho, and Michael A. Saunders, *Atomic decomposition by basis pursuit*, SIAM Journal on Scientific Computing **20** (1998), 33–61.
- [20] David Donoho and Jared Tanner, *Neighborliness of randomly projected simplices in high dimensions*, Proc. Natl. Acad. Sci. USA **102** (2005), 9452–9457.
- [21] David Donoho, *Compressed sensing*, IEEE Trans. Inform. Theory **52** (2006), 1289–1306.
- [22] Bradley Efron, Trevor Hastie, Iain Johnstone, and Robert Tibshirani, *Least angle regression*, Annals of Statistics **32** (2004), 407–499.
- [23] Ernie Esser, Xiaoqun Zhang, and Tony F. Chan, *A general framework for a class of first order primal-dual algorithms for convex optimization in imaging science*, SIAM J. Imaging Sci. **3** (2010), no. 4, 1015–1046.
- [24] Albert C. Fannjiang, *Exact localization and superresolution with noisy data and random illumination*, Inverse Problems **27** (2011), no. 6, 065012.
- [25] Mario A. T. Figueiredo and Robert D. Nowak, *An EM Algorithm for Wavelet-Based Image Restoration*, IEEE Transactions on Image Processing **12** (2003), 906–916.
- [26] Mario A. T. Figueiredo, Robert D. Nowak, and Stephen J. Wright, *Gradient projection for sparse reconstruction: application to compressed sensing and other inverse problems* **1** (2007), 586–597.
- [27] Michel Fortin and Roland Glowinski, *Augmented Lagrangian methods*, Studies in Mathematics and its Applications, vol. 15, North-Holland Publishing Co., Amsterdam, 1983. Applications to the numerical solution of boundary value problems; Translated from the French by B. Hunt and D. C. Spicer.
- [28] Tom Goldstein and Stanley Osher, *The Split Bregman Method for L1-Regularized Problems*, SIAM J. Img. Sci. **2** (2009), 323–343, DOI 10.1137/080725891.
- [29] Magnus R. Hestenes, *Multiplier and gradient methods*, J. Optimization Theory Appl. **4** (1969), 303–320.
- [30] Bing Jian and Baba C. Vemuri, *A unified computational framework for deconvolution to reconstruct multiple fibers from diffusion weighted MRI*, IEEE Trans. Medical Imaging **26** (2007), 1464–1471.
- [31] Narendra Karmarkar, *A new polynomial-time algorithm for linear programming*, Combinatorica **4** (1984), 373–395.
- [32] Seung-Jean Kim, Kwangmoo Koh, Michael Lustig, Stephen Boyd, and Dimitry Gorinevsky, *A method for large-scale ℓ_1 -regularized least squares problems with applications in signal processing and statistics*, IEEE Journal on Selected Topics in Signal Processing **1** (2007), 606–617, available at www.stanford.edu/boyd/11_ls.html.
- [33] Michael Lustig, David Donoho, and John M. Pauly, *Sparse MRI: The application of compressed sensing for rapid MR imaging*, Magnetic Resonance in Medicine **58** (2007), 1182–1195.
- [34] Yu E. Nesterov, *A method of solving a convex programming problem with convergence rate $O(1/k^2)$* , Soviet Mathematics Doklady **27** (1983), 372–376.
- [35] ———, *Gradient methods for minimizing composite objective function*, Technical Report 2007076, Universit catholique de Louvain, Center for Operations Research and Econometrics (CORE), 2007, <http://econpapers.repec.org/RePEc:cor:louvco:2007076>.

- [36] M.R. Osborne, B. Presnell, and B.A. Turlach, *A new approach to variable selection in least squares problems*, IMA Journal of Numerical Analysis **20** (2000), no. 3, 389–403, DOI 10.1093/imanum/20.3.389.
- [37] Stanley Osher, Martin Burger, Donald Goldfarb, Jinjun Xu, and Wotao Yin, *An iterative regularization method for total variation-based image restoration*, Multiscale Model. Simul. **4** (2005), 460–489.
- [38] M. J. D. Powell, *A method for nonlinear constraints in minimization problems*, Optimization (Sympos., Univ. Keele, Keele, 1968), Academic Press, London, 1969, pp. 283–298.
- [39] H. Raguét, J. Fadili, and P. Peyre, *Generalized Forward-Backward Splitting*, Preprint (2011).
- [40] R. Tyrrell Rockafellar, *A dual approach to solving nonlinear programming problems by unconstrained optimization*, Math. Programming **5** (1973), 354–373.
- [41] Guillermo Sapiro, *Geometric partial differential equations and image analysis*, Cambridge University Press, Cambridge, 2001.
- [42] Emil Y. Sidky, Chien-Min Kao, and Xiaochuan Pan, *Accurate image reconstruction from few-views and limited-angle data in divergent-beam CT*, J. X-ray Sci. Technol. **14** (2006), 119–139.
- [43] Emil Y. Sidky and Xiaochuan Pan, *Image reconstruction in circular cone-beam computed tomography by constrained, total-variation minimization*, Physics in Medicine and Biology **53** (2008), no. 17, 4777.
- [44] Robert Tibshirani, *Regression shrinkage and selection via the Lasso*, Journal of the Royal Statistical Society, Series B **58** (1994), 267–288.
- [45] Yaakov Tsaig and David Donoho, *Extensions of compressed sensing*, Signal Processing **86** (2005), 533–548.
- [46] Margaret H. Wright, *The interior-point revolution in optimization: history, recent developments, and lasting consequences*, Bull. Amer. Math. Soc. (N.S) **42** (2005), 39–56.
- [47] Wotao Yin, Stanley Osher, Donald Goldfarb, and Jerome Darbon, *Bregman iterative algorithms for ℓ_1 -minimization with applications to compressed Sensing*, SIAM J. on Imaging Sciences **1** (2008), 143–168.
- [48] Wotao Yin, *Analysis and generalizations of the linearized Bregman model*, SIAM J. Imaging Sci. **3** (2010), no. 4, 856–877.